Study of Electromagnetic Shielding for Reduction of Magnetic Fields Generate by Underground Power Cables via a Finite Element Techinique

Hung Bui Duc, Truong Cong Trinh, Minh Quan Duong, Vuong Dang Quoc*

Abstract—Nowadays, with the development of the industries, the electrical types of equipments are used and applied widely for many different fields and purposes. One of them is the use of power cable systems to transmit and distribute electricity over long distances, from generator stations to consumers. As we have known, magnetic fields are usually generated by the presence of a single or three phase current following in power cable systems in general and underground power cables in particular. Not only causes directly some unwanted effects on the body's natural equilibrium, but electromagnetic fields can create the disturbance and cause interference with electronic devices. In this context, to mitigate/reduce distribution of electromagnetic fields generated by a three phase current of underground power cables, an electromagnetic shielding with the different materials is proposed to get overcome above drawbacks. The computation of magnetic fields is implemented via a finite element technique with the development of magnetic vector potential formulations. The developed method is applied to a practical problem.

Index Terms—Electromagnetic shieldings; magetic fields, underground power cables; finite element approach; magnetic vector potential formulations.

1. Introduction

THE influence of health due to magnetic fields is a big matter, which needs to be greatly concerned. Recently, many research activities and laboratory studies have been deeply discussed about underground power cables, such as [1]- [4]. In [1], authors have proposed a protective solution for underground power cables for an actual distribution grid according to IEEE standards. In [2]- [4], the papers studied the effection of the magnetic fields on the human body. They have shown that the tissues of the body are able to protect and therefore mitigate the affects of electric fields. But, the tissues cannot shield the magnetic fields, and thus do not decrease their effects. , the direct effection of electromagnetic fields to the body is presented by the electric current density (A/m^2) with the different values. When the current density (J) (mA/m^2) is defined as $1 < J < 10$, $10 < J < 100$ and $100 < J < 1000$, the symptoms that may appear respectively are minor effects, possible symptoms on the nervous system, tissues stimulation: possible risks, symptoms extrasystoles and fibrillation [5]. Hence, researchers have been still studying and finding possible techniques to reduce magnetic fields. There are many types of sources of magnetic fields, and it is still a big challenge for researchers to manage these fields. One of these sources is the underground power cables, what are often used for electrical systems in general and industrial in particular. Several methods have been proposed to reduce the magnetic fields, that is, "intrinsic methods" and "extrinsic methods" [6]-[8]. In the both of two methods, the cable parameters are arranged in a suitable way for mitigation of electromagnetic fields. Or external shieldings can be made of ferromagnetic or conductive materials and grids of insulated conductors [8]- [14]. All the techniques have advantages and drawbacks, but this paper will focus on extrinsic techniques by using multi-layered shielding for underground power cables. To achieve the best shield configuration, some cases are proposed and compared. A finite element method (FEM) is extended with the development of magnetic vector potential formulations to investigate and analyse the magnetic field distributions generated by underground power cables with several cases. The obtained results will be shown that the influence of arrangements of the electromagnetic shieldings with different materials on the magnetic field distribution due to underground power cables. Reduction factors of their proximities are also considered in

Hung Bui Duc, Truong Cong Trinh and Vuong Dang Quoc are with the School of Electrical and Electronic Engineering, Hanoi University of Science and Technology (E-mail: hung.buiduc@hust.edu, trinh.tc222025m@sis.hust.edu.vn, vuong.quoc@hust.edu.vn).

Minh Quan Duong is with the University of Danang - University of Science and Technology, Danang, Vietnam (E-mail: dmquan@dut.udn.vn).

**Corresponding author: Vuong Dang Quoc (E-mail: vuong.quoc@hust.edu.vn)*

Manuscript received October 09, 2022; revised November 10, 2022; accepted December 05, 2022.
Digital Object Identifier 10.31130/ud-jst.2022.478ICT

this paper.

2. Electromagnetic shielding

The influence of magnetic fields due to the sources on public health is concerned. A number of design solutions has been proposed to reduce the magnetic field in a certain region. Depending on the protection purposes, they could be classified into two categories: shielding a subject and shielding a source. In some places such as laboratories, and some kinds of the factory where equipment needs the high accuracy, they can be shielded individually. Protecting a subject contains the implementation of some kind of shield to decrease the magnetic field of outside field sources in some comparatively small volume. Meanwhile, a source is shielded when we place a shield in the surrounding source area to reduce the magnetic field that leaked to the outside. However, in most cases, a shielding source, which is the underground power cables, is more general and cost-effective. In this paper, electromagnetic shields are made of two different materials with the high electrical conductivity and magnetic permeability are used to achieve the mitigation of the magnetic flux density. For the material with high electrical conductivity, it becomes the site of the eddy current due to the magnetic field distribution, whereas the material with high magnetic permeability is the site of magnetic field concentration. For that, it will shield the influence of magnetic fields in the around areas. In addition, the combination of the magnetic and conductive materials is considered as good shielding capacities [5]. In order to evaluate and compare the magnetic field reduction ability of different types of electromagnetic shields, this paper uses a reduction factor (or shielding factor) (RF), which is the ratio of magnetic flux density without the shield (B_0) to the magnetic flux density with the shield (B_s). Thus, the RF can be defined as:

$$RF = \frac{B_0}{B_s} \tag{1}$$

From the expression (1), we have seen that the bigger the RF value is, the better the magnetic field reduction. In this paper, the material with high electrical conductivity is copper and the material with high magnetic permeability is M-6 CARLITE [15]. The simulation results are then compared with the data from [5].

3. Weak finite element formulations

3.1. General magnetodynamic model

A magnetodynamic model is defined in a domain Ω, where the boundary $\partial\Omega$ is defined as $\partial\Omega = \Gamma = \Gamma_h \cup \Gamma_b$. The Maxwell's equations with constitute laws are presented in a studied domain Ω [16]- [17]. The Maxwell's equations with constitute laws are presented in a studied domain $\partial\Omega$ [16]- [17].

$$\text{curl}\, \boldsymbol{H}_n = j_s,\ \text{curl}\, \boldsymbol{E}_n = -\partial_t \boldsymbol{B}, \text{div}\, \boldsymbol{B}_n = 0 \quad \text{(2a-b-c)}$$

$$\boldsymbol{B} = \mu_n \boldsymbol{H}\,,\ \boldsymbol{J} = \sigma \boldsymbol{E} \tag{3a-b}$$

Where:

- $\boldsymbol{H}$: the the magnetic field (A/m),
- $\boldsymbol{B}$: the magnetic flux density (T),
- $\boldsymbol{J}_s$: the electric current density (A/m2),
- $\boldsymbol{E}$: the electric field (V/m),
- σ: the electric conductivity (S/m).
- μ: the relative permeability.

The boundary conditions (BCs) are determined on γ, that is,

$$\boldsymbol{n} \cdot \boldsymbol{B}|_{\Gamma_e} = 0\,,\ \boldsymbol{n} \times \boldsymbol{H}|_{\Gamma_h} = 0\,, \tag{4a-b}$$

where n is the unit normal exterior to Ω [16]. The domain Ω is divided into two parts, i.e., Ω_c and $\Omega_{c,n}^C$, where Ω_c is the conducting region and $\Omega_{c,n}^C$ is the non-conducting region. The equations (3 a) and (3 b) are solved with the BCs already given from (4 a-b) taking the normal and tengential components of $\boldsymbol{B}$ and $\boldsymbol{H}$ into account. The local fields of $\boldsymbol{H}, \boldsymbol{B}, \boldsymbol{E}$ and $\boldsymbol{J}$ are determined to satisfy Tonti's diagram [16], [17].

3.2. Weak form of magnetic vector potential formulations

Based on the set of Maxwell's equations (2 a-b-c) and the constitutive laws (2 a-b), the magnetic vector potential weak formulation is written as

$$\boldsymbol{B} = \text{curl}\, \boldsymbol{A}, \tag{5}$$

In order to exactly satisfy the Ampere's law (2 a) and the behavior law (3 a), the fields of $\boldsymbol{H}$ and $\boldsymbol{J}$ belong to the function spaces $\boldsymbol{H}_h(\text{curl};\Omega)$, $\boldsymbol{H}_h(\text{div};\Omega)$). This means that the field b belongs to $\boldsymbol{H}_h(\text{curl};\Omega)$, i.e. $\boldsymbol{B} \in \boldsymbol{H}_h(\text{curl};\Omega)$.

By substituting the equation (5) into equation (5 c), the field of $\boldsymbol{E}$ is presented via an electric scalar potential ϕ, i.e.

$$\boldsymbol{E} = -j\omega \boldsymbol{A} = \text{grad}\, \phi \tag{6}$$

From the equations (4), (5) and (6), the weak formulation is defined via the Ampère equation (2 a) and the constitutive law (3 a). Hence, one has

$$\oint_\Omega \mu^{-1} \boldsymbol{B} \cdot \text{curl}\, \boldsymbol{A} d\Omega + \oint_\Omega \sigma \boldsymbol{E} \cdot \boldsymbol{A}' d\Omega_c + \int_{\Gamma_h} \boldsymbol{n} \times \boldsymbol{H} \cdot \boldsymbol{A}' d\Gamma_h = \oint_\Omega \boldsymbol{J}_s \cdot \boldsymbol{A}' d\Omega_s\,, \boldsymbol{A}' \in \boldsymbol{H}_h^1(\text{curl};\Omega) \tag{7}$$

By substituting (5) and (6) into (3.2), one gets [17]

$$\oint_\Omega \mu^{-1} \text{curl}\, \boldsymbol{A} \cdot \text{curl}\, \boldsymbol{A}' d\Omega + j\omega \oint_\Omega \sigma \boldsymbol{A} \cdot \boldsymbol{A}' d\Omega_c + j\omega \oint_\Omega \sigma \text{grad}\, \phi \cdot \boldsymbol{A}' d\Omega_c + \int_{\Gamma_h} \boldsymbol{n} \times \boldsymbol{H} \cdot \boldsymbol{A}' d\Gamma_h = \oint_\Omega \boldsymbol{J}_s \cdot \boldsymbol{A}' d\Omega_s\,, \boldsymbol{A}' \in \boldsymbol{H}_h^1(\text{curl};\Omega) \tag{8}$$

Note that the function space $\boldsymbol{H}_h^1(\text{curl};\Omega)$ containing the test function $\boldsymbol{A}'$ and basis functions a is a defined in Ω.

3.3. Field discretizations

In (3.2) and (3.2), the field a is discretized by node and edge elements, i.e. [16]

$$\boldsymbol{A} = \sum_{e\in E(\Omega_c^C)\setminus e(\partial\Omega_c)} a_e s_e + \sum_{e\in E(\Omega_c)} a_e s_e. \quad (9)$$

$$\phi_s = \sum_{n\in N(\Gamma_h)} \phi_n. \quad (10)$$

The elements $E(\Omega_c$ and $E(\Omega_c^C$ in (9) and (10) are the set of edges of Ω, s_e is the basis function of edge, and a_e is the circulation of a along the edge e. The element $N(\Gamma_h)$ in (refeq10) is all the nodes of the BCs. By substituting (3.2) and (9) into (10), one is rewritten as:

$$\oint_\Omega (\sigma \sum_{e\in E(\Omega_c)} a_e s_e \cdot \text{grad}\,\phi_s) d\Omega +$$
$$\oint_\Omega (\sigma \sum_{e\in E(\Omega_c^C)\setminus e(\partial\Omega_c)} a_e s_e \cdot \text{grad}\,\phi_s) d\Omega +$$
$$j\omega \oint_\Omega (\sigma \sum_{n\in N(\Gamma_h)} \text{grad}\,\phi_n \cdot \text{grad}\,\phi_s) d\Omega$$
$$= \oint_\Omega \boldsymbol{J}_s \cdot \boldsymbol{A}' d\Omega_s \,, \boldsymbol{A}' \in \boldsymbol{H}_h^1(\text{curl}\,;\Omega) \quad (11)$$

4. Numerical simulation

The test problem is shown in Fig. 1. It consists of an electromagnetic shielding located above the underground power cables. The length of the shielding plate is 1000 mm, the phase-to-phase distance is 125 mm, and the distance between the shielding plate and power cables is 200 mm. The values of balanced current and frequency are given 100 A and f = 50 Hz, respectively.

First, the problem is tested without a shield. The magnetic flux density measurement points are at the height of 300 mm, 400 mm, 500 mm, 600 mm, and 700 mm from the cables as presented in Fig. 1 (bottom). The simulation result for different points is pointed out in Fig. 2.

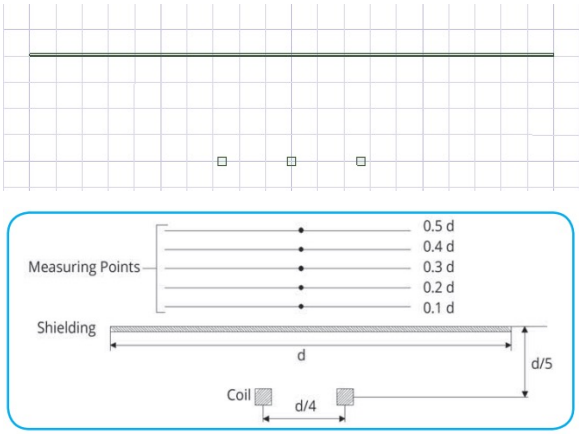

Fig. 1: 2D-Geometry model [5].

Next, the cases are simulated to measure and compare the results between them.

Case1: The shield with high electrical conductivity facing the source In this case, the total thickness of the shield is equal to 4.7 mm with layers having the following features (3).

- 1st layer: M-6 steel composed of two overlaid plates each 0.35 mm thick.
- 2nd layer: copper with the thickness of 4 mm.

The magnetic vector potential distribution is presented in Fig. 4, for the permeability of the copper shield (μ_n), μ_n = $1,2566.10^6$ H/m. It can be seen that the flux lines are deflected when they first come into contact with the surface of the shield. The flux density is measured at different points as mentioned above. The distribution of eddy current in the shielding is indicated in Fig. 5. Its value is very high at the corner due to the skin effect. Fig. 6 shows the flux density value computed along the lines which have the length equal to the shield at the height of the measurement points. The results of the reduction factor with the simulation and measurement are presented in Fig. 7. The errors on two methods are lower than 5%.

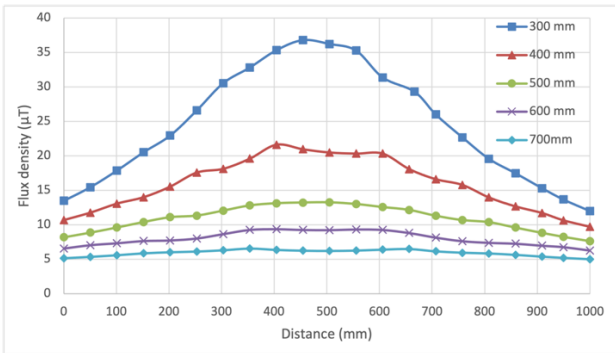

Fig. 2: Distribution of magnetic flux densities along the lines at the different measuring points without a shield.

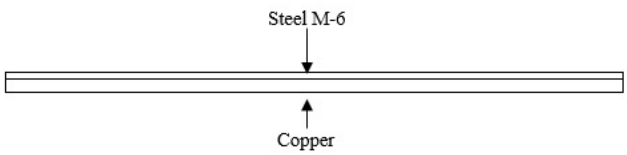

Fig. 3: Electromagnetic shielding with copper facing source.

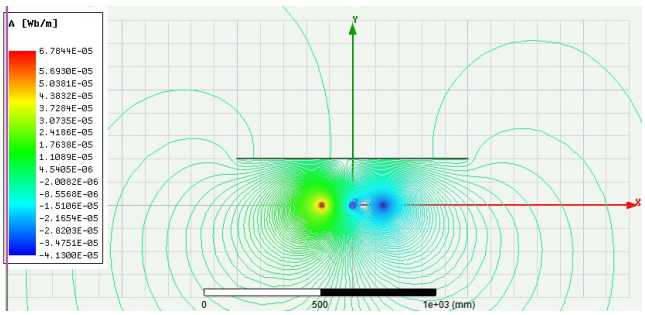

Fig. 4: Flux line distribution on magnetic vector potential.

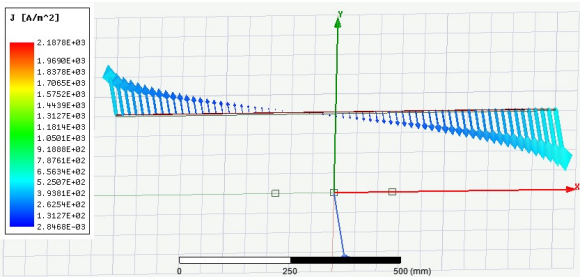

Fig. 5: Eddy current density distribution in the shield.

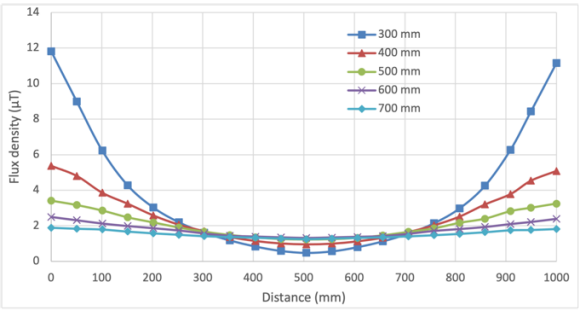

Fig. 6: Distribution of magnetic flux densities along the lines at the different measuring points without the shield.

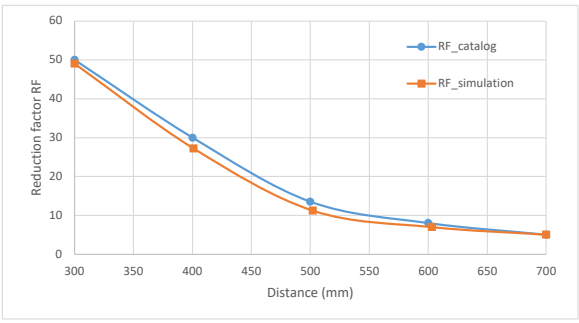

Fig. 7: Reduction factors with the FEM and measured method.

Case 2: The shield with high magnetic permeability facing the source The overall thickness of the shield is still equal to 4.7 mm, but the positions of the layers are reversed for each other. The layer with steel M-6 faces the source as shown in Fig. 8. In the same way, the distribution of flux line on magnetic vector potential is pointed out in Fig. 9 with a affects of properties of the shielding. The eddy current density distribution in the shield is also presented in Fig. 10. Its value is very big at the shielding end.

In addition, for this case, it can be seen that because the steel M-6 plate faces the source, the majority of the flux is absorbed, especially at the part near the two ends of the shield. Thus, the current density at those positions is larger. By comparing the two cases, the current density value in case 2 is 25 times the one in case 1. Hence, it is clear that the field configuration in case 2 is better. This is further clarified when comparing the results of the flux density and the reduction factor between the two cases. The flux density distributions at different measurement points is presented in Fig. 11. The values are the smallest with the distance of measured point of 700 mm, and the larggest with the distance of measured point of 300 mm. In the same way to case 1, the reduction factors with the FEM and measured method is shown in Fig. 12. The errors between two methods are lower than 7%. The results of the actual measurement from [5] concluded that the shield configuration in case 2 can reduce the magnetic field better than the one in case 1 as pointed out in Fig. 7. In addition, in case 1, the maximum reduction factor value is just 40, whereas it is 75 in case 2. As mentioned above, the data from the simulation is quite different from the actual measurement data. This is due to the difference in the materials used and the simulation software can not consider the external conditions that affect the actual measurement.

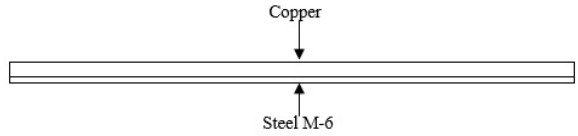

Fig. 8: Electromagnetic shielding with the steel M-6 facing source.

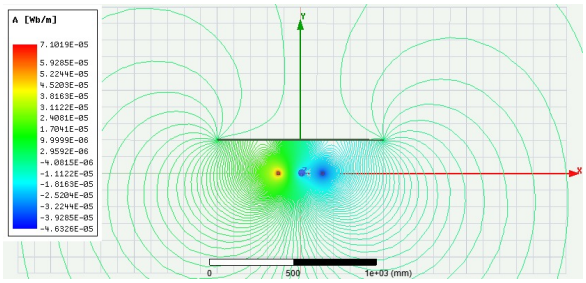

Fig. 9: Flux line distribution on magnetic vector potential.

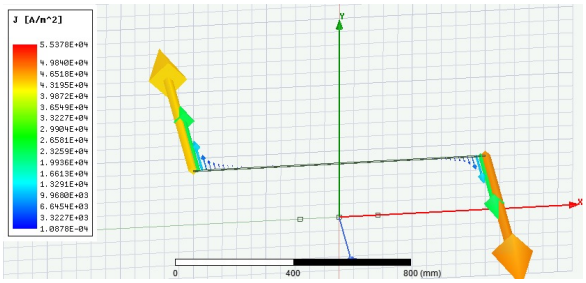

Fig. 10: Distribution of eddy current density in the shield.

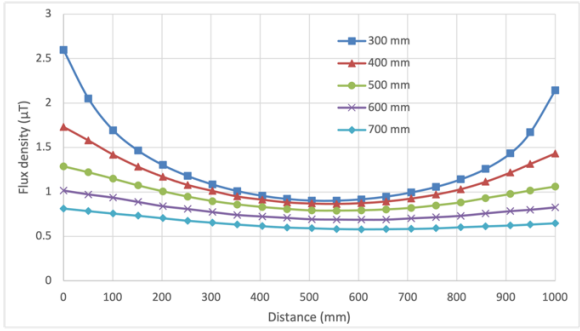

Fig. 11: Flux density distributions at different measurement points.

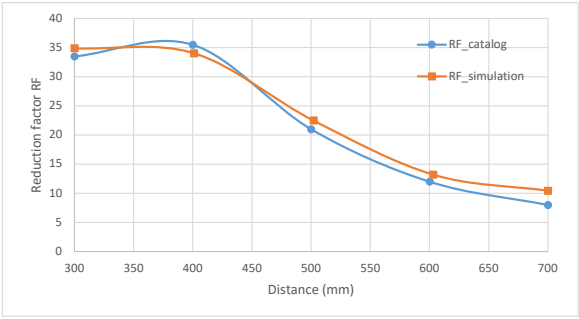

Fig. 12: Reduction factors with the FEM and measured method.

5. Conclusions

In this paper, based on the finite element technique with the development of magnetic vector potential, the authors have successfully proven the better configuration of the shield to reduce the magnetic fields. With the same materials, the electromagnetic shielding with the steel M-6 plate facing the source can absorb the magnetic field better than the one with the copper plate facing the source. For the obtained results, they can help the manufacturers and researchers to give the suitable choice of the electromagnetic shielding configuration for other applications of the underground power cables.

For the obtained results from the proposed method, this is a good agreement for extending to the magnetic field intensity formulations for the future work.

Acknowledgment

This research is funded by Hanoi University of Science and Technology under project number T2022-PC-009.

References

[1] Hieu, Trinh Trung and Vinh, Tran Tan and Duong, Minh Quan and Khoa Nam, Nguyen Nhu and Sava, Gabriela Nicoleta, "Analysis of Protective Solutions for Underground Cable System - Application for Danang Distribution Grid," *10th International Conference on ENERGY and ENVIRONMENT (CIEM).*, pp.1-5, 2021. Doi=10.1109/CIEM52821.2021.9614812.

[2] McKinlay AF, Allen SG, Cox R, Dimbylow PJ, Mann SM, Muirhead CR, Saunders RD, Sienkiewicz ZJ, Stather JW, Wainwright PR, "Review of the Scientific Evidence for Limiting Exposure to Electromagnetic Fields (0-300 GHz)," *National Radiological Protection Board (NRPB).*, Vol.15, No.3: 1-224, ISBN 978-0-85951-533-7.

[3] HASSAN A. KALHOR and MOHAMMAD R. ZUNOUBI, "Mitigation techniques of power frequency magnetic fields originated from electric power systems, International Council on Large Electric Systems," *Taylor and Francis. Electromagnetics.* , Vol. 25, no. 3, pp. 231–243, 2005. Doi = 10.1080/02726340590915610.

[4] H. B. Duc, T. P. Minh, D. B. Minh, N. P. Hoai, and V. D. Quoc, "An Investigation of Magnetic Field Influence in Underground High Voltage Cable Shields," *Eng. Technol. Appl. Sci. Res.*, vol. 12, no. 4, pp. 8831–8836, 2022. Doi = 10.48084/etasr.5021.

[5] A. Canova, L. Giaccone, G. Lavecchia and P. Ribaldone, "Passive mitigation of stray magnetic fields generated by underground power lines," *2017 IEEE International Conference on Environment and Electrical Engineering and 2017 IEEE Industrial and Commercial Power Systems Europe*, pp. 1-5, 2017. Doi = 10.1109/EEEIC.2017.7977522.

[6] Satis Shielding, "Electromagnetic shielding products," [Online] Available: https://www.beshielding.com.

[7] E. Mimos, D. Tsanakas, and A. Tzinevrakis, "Optimum phase configurations for the minimization of the magnetic fields of underground cables," *Electr. Eng.*, vol. 91, pp. 327–335, 2010. Doi = 10.1007/s00202-009-0126-x.

[8] Machado, Vitor, "Magnetic Field Mitigation Shielding of Underground Power Cables," *Magnetics, IEEE Transactions on.*, vol. 48, pp. 707–710, 2012. Doi = 110.1109/TMAG.2011.2174775.

[9] C.del Pino López, P.Cruz Romero, P.Dular, "Parametric analysis of magnetic field mitigation shielding for underground power cables," *RE and PQJ.*, vol. 01, no.5, pp. 519–526, 2012. Doi = 110.24084/repqj05.326.

[10] M. E. Almeida, V. M. Machado, and M. G. Neves "Mitigation of the magnetic field due to underground power cables using an optimized grid," *Eur. Trans. Electr. Power*, vol. 21, pp. 180–187, 2011. Doi = 110.24084/repqj05.326.

[11] T. Barbarics, A. Kost, D. Lederer, and P. Kis, "Electromagnetic field calculation for magnetic shielding with ferromagnetic material," *IEEE Trans. Magn.*, vol. 36, no. 4, pp. 986–989, 2000. Doi = 10.1109/20.877607.

[12] K. Yamazaki, K. Muramatsu, M. Hirayama, A. Haga, and F. Torita, "Optimal structure of magnetic and conductive layers of a magnetically shielded room," *IEEE Trans. Magn.*, vol. 42, no. 10, pp. 3524–3526, 2006. Doi = 10.1109/20.877607.

[13] M. D'Amore, E. Menghi and M. S. Sarto, "Shielding techniques of the low-frequency magnetic field from cable power lines," *2003 IEEE Symposium on Electromagnetic Compatibility. Symposium Record (Cat. No.03CH37446)*, 2003, pp. 203-208 vol.1. Doi = 10.1109/ISEMC.2003.1236592.

[14] CIGRE, Work Group on Electric Power Systems, WG C4.204, "Mitigation techniques of power-frequency magnetic fields," *Electra*, vol.242, pp. 75–83, Feb.2009.

[15] A. Farag, M. Dawoud, and I. Habiballah, "Implementation of shielding principles for magnetic field management of power cables," *Electric Power Syst. Res.*, vol. 48, pp. 193–209, 1999.

[16] A. Farag, M. Dawoud, and I. Habiballah, "Implementation of shielding principles for magnetic field management of power cables," *Electric Power Syst. Res.*, vol. 48, pp. 193–209, 1999.

[17] Vuong Q. Dang, P. Dular, R. V. Sabariego, L. Krähenbühl and C. Geuzaine, "Subproblem Approach for Thin Shell Dual Finite Element Formulations," *IEEE Trans. Magn.*, vol. 48, no. 2, pp. 407–410, 2012.

[18] S. Koruglu, P. Sergeant, R.V. Sabarieqo, Vuong. Q. Dang, M. De Wulf, "Influence of contact resistance on shielding efficiency of shielding gutters for high-voltage cables," *IET Electric Power Applications*, Vol.5, No.9, (2011), pp. 715-720.

Hung Bui Duc received the PhD degree in 2000 from Department of Electrical Engineering, Hanoi University of Science and Technology. He is currently working as a team leader of electrical machines's group, and also a lecturer of Department of Electrical Engineering, School of Electrical Engineering, Hanoi University of Science and Technology, no1 Dai Co Viet Street, Hai Ba Trung District, Ha Noi.

Truong Cong Trinh received the Engineer degree in 2021 from Department of Electrical Engineering, Hanoi University of Science and Technology. He is currently working as a master thesis of Department of Electrical Engineering, School of Electrical Engineering, Hanoi University of Science and Technology, no1 Dai Co Viet Street, Hai Ba Trung District, Ha Noi.

Minh Quan Duong is currently a lecturer at the Department of Electrical Engineering, The University of Danang - University of Science and Technology, 54 Nguyen Luong Bang St., Lien Chieu District, Danang city, Vietnam.

Vuong Dang Quoc received his PhD degree in 2013 from the Faculty of Applied Sciences at the University of Liege in Belgium. After that he came back to the Hanoi University of Science and Technology in September 2013, where he is currently working as a lecturer of Department of Electrical and Electronic Equipment, School of Electrical Engineering, Hanoi, University of Science and Technology. His research domain encompasses modeling of electromagnetic systems by coupling of subproblem method with application to thin shell models.